Biosensors and Bioelectronics 231 (2023) 115284

Contents lists available at ScienceDirect

Biosensors and Bioelectronics

journal homepage: www.elsevier.com/locate/bios

A lab-on-a-chip utilizing microwaves for bacterial spore disruption and detection

Shayan Valijam [a,b,1], Daniel P.G. Nilsson [b,1], Rasmus Öberg [b], Unni Lise Albertsdóttir Jonsmoen [c], Adrian Porch [d], Magnus Andersson [b,e,*], Dmitry Malyshev [b,**]

[a] Faculty of Electrical Engineering, K. N. Toosi University of Technology, Tehran, 1631714191, Iran
[b] Department of Physics, Umeå University, Umeå, 901 87, Sweden
[c] Department of Paraclinical Sciences, Faculty of Veterinary Medicine, Norwegian University of Life Sciences, Ås, 1433, Norway
[d] School of Engineering, Cardiff University, Cardiff, CF24 3AA, United Kingdom
[e] Umeå Center for Microbial Research (UCMR), Umeå, 901 87, Sweden

ARTICLE INFO

Keywords:
Raman spectroscopy
Fluorescence sep CaDPA
Waveguide
Biomarker
Bacillus

ABSTRACT

Bacterial spores are problematic in agriculture, the food industry, and healthcare, with the fallout costs from spore-related contamination being very high. Spores are difficult to detect since they are resistant to many of the bacterial disruption techniques used to bring out the biomarkers necessary for detection. Because of this, effective and practical spore disruption methods are desirable. In this study, we demonstrate the efficiency of a compact microfluidic lab-on-chip built around a coplanar waveguide (CPW) operating at 2.45 GHz. We show that the CPW generates an electric field hotspot of ~10 kV/m, comparable to that of a commercial microwave oven, while using only 1.2 W of input power and thus resulting in negligible sample heating. Spores passing through the microfluidic channel are disrupted by the electric field and release calcium dipicolinic acid (CaDPA), a biomarker molecule present alongside DNA in the spore core. We show that it is possible to detect this disruption in a bulk spore suspension using fluorescence spectroscopy. We then use laser tweezers Raman spectroscopy (LTRS) to show the loss of CaDPA on an individual spore level and that the loss increases with irradiation power. Only 22% of the spores contain CaDPA after exposure to 1.2 W input power, compared to 71% of the untreated control spores. Additionally, spores exposed to microwaves appear visibly disrupted when imaged using scanning electron microscopy (SEM). Overall, this study shows the advantages of using a CPW for disrupting spores for biomarker release and detection.

1. Introduction

Detection of pathogenic bacteria is important in many parts of society, from agriculture and food industries where contamination leads to huge financial costs (Osimani et al., 2018), to healthcare and homeland security where bacterial detection can be a matter of life and death (Goel, 2015). Some bacteria form resilient endospores when exposed to adverse conditions. Spore-forming bacteria are associated with serious hospital-acquired infections (*Clostridioides difficile*) (Wang et al., 2015b) and contamination of food (*Bacillus cereus*, *Clostridium botulinum*) (Andersson et al., 1998), some are even classified as biohazard agents (*Bacillus anthracis*) (Manchee et al., 1983). Due to their resilience and the hazard they present, the detection of bacterial spores is of particular importance. Spores are especially difficult to detect due to their chemical resistance and structural robustness, with their DNA and other internal biomarkers shielded by multiple protective spore layers (Stewart, 2015). Thus, detection using conventional microbiological techniques such as polymerase chain reaction is often slow and ineffective, either requiring the spores to germinate into their vegetative cell form or using an aggressive chemical treatment to cause spore disruption (Pellegrino et al., 2002; de Bruin et al., 2019).

One proposed method to disrupt spores and release biomarkers for

* Corresponding author. Department of Physics, Umeå University, Umeå, 901 87, Sweden.
** Corresponding author.
E-mail addresses: magnus.andersson@umu.se (M. Andersson), dmitry.malyshev@umu.se (D. Malyshev).
URL: https://www.umu.se/en/research/groups/the-biophysics-and-biophotonics-group/ (M. Andersson).
[1] Contributed equally to the work.

https://doi.org/10.1016/j.bios.2023.115284
Received 4 January 2023; Received in revised form 7 March 2023; Accepted 28 March 2023
Available online 31 March 2023

detection is exposing them to high-power microwave radiation. Microwaves are a common, reliable, and efficient way to deliver energy to an organic sample (Sorrentino and Bianchi, 2010). In a spore sample, microwaves can induce spore breakdown by means of both thermal and non-thermal effects (Celandroni et al., 2004; Kim et al., 2009). Breaking down spores releases the spore DNA (Aslan et al., 2008) and calcium dipicolinic acid (CaDPA) (Celandroni et al., 2004) contained in the spore core, the latter being a protective chemical known to shield the spore core from wet heat (Kong et al., 2012). CaDPA is also a spectroscopic spore biomarker that provides a unique Raman spectral fingerprint and a fluorescence emission signal, which varies between weak and strong depending on the environmental conditions (Malyshev et al., 2022c; Sarasanandarajah et al., 2005). Previous studies have shown that spores can be broken down using microwave applicators. This includes specialized devices (Malyshev et al., 2019), but also regular commercial microwave ovens (Vaid and Bishop, 1998). However, these devices are excessively large for microbiological samples that are on the μl to ml scale and are not convenient in field sampling assays. Thus, there is a need for the development of compact microwave applicators where small-scale experiments can be performed in a lab-on-a-chip environment.

A promising method to deliver localised microwave irradiation into small-scale samples is via coplanar waveguides (CPWs). CPWs are electrical planar transmission lines imprinted in a thin metal layer on top of a dielectric substrate (Simons, 2004). These are commonly made on printed circuit boards (PCB) (Wen, 1969), making it possible to combine CPWs with signal processing circuitry to create more complex devices (Abduljabar et al., 2017; Williams et al., 2018). Another benefit of CPWs, is the high-power microwaves they can produce at wavelengths suitable for biological applications. At these wavelengths, the CPW chip is only a few cm across, making it ideal for irradiating small-scale biological samples.

A coplanar waveguide lab-on-a-chip design can be used in conjunction with various detection techniques to create effective and portable detection assays, and a number of devices are being developed for various medical monitoring (Vashist et al., 2015). Conventional biological techniques can use DNA to directly detect spores (or other microbiological samples), but the amount of DNA is small, and laboratory methods such as PCR are needed to amplify the signal (Belgrader et al., 1999). However, when using CaDPA as a biomarker, there exists a plethora of spectroscopic techniques for detecting spores. This includes Raman spectroscopy and Raman subtechniques such as surface enhanced Raman spectroscopy (SERS) (Kočišová and Procházka, 2018; Zhang et al., 2005). It also includes various photoluminescence and fluorescence-based techniques, often utilizing either ultraviolet radiation (Sarasanandarajah et al., 2005), or terbium-based nanostructures (Li et al., 2013), to enhance the naturally low fluorescence of CaDPA as a spore biomarker.

The aim of this work is to develop a lab-on-a-chip device to disrupt bacterial spores in aqueous suspension for small-scale biosensing applications, as illustrated in Fig. 1. The device uses a microfluidic channel to transport spores through a high electric field (E) region in a CPW operated at 2.45 GHz. The microwave exposure disrupts the spores, causing them to release their core content, including CaDPA, into the suspension. The released CaDPA can subsequently be detected using both spectroscopic or non-spectroscopic detection techniques. As a proof of concept, we tested ml-volume samples of diluted *Bacillus thurigensis* spores in our CPW applicator and analyzed the suspension using fluorescence spectroscopy. To assess the chemical change on individual spores, we utilized Laser Tweezer Raman spectroscopy (LTRS). We found that significant spore disruption is achieved at microwave powers as low as ~1 W. This corresponds to an applied electric field strength of around $\sim 10^4$ V/m, similar to that of a commercial microwave oven (Monteiro et al., 2011). These results show the potential of using CPW applicators in compact lab-on-a-chip devices for spore disruption and detection assays.

2. Material and methods

2.1. Coplanar waveguide theory and design

In a microwave system, the applicator is the part that applies an electric field to a sample by acting as an antenna. Applicators are generally classified as resonant or non-resonant, and can be based on either transmission lines or waveguides. The benefit of a resonant microwave applicator is the high electric and magnetic (EM) fields for a given input power, magnified by the high-quality factor (Q) of the applicator's resonant cavity or transmission line. However, a high Q resonant applicator is intrinsically tuned to have a narrow bandwidth resonant response. As such, it has to be excited very close to its resonant frequency for maximum output. This means that resonant microwave applicators become detuned with an aqueous sample placed in a region of high electric field due to the high dielectric loss of water, with further losses due to the reduction in Q. This effect becomes even more pronounced for electrolytic samples at radio and low microwave frequencies (0.1–3 GHz). Additionally, the strong temperature dependence of relative permittivity in a water sample results in a reduction in the applicator's resonant frequency if the sample temperature increases with microwave exposure. For these reasons, there has to be continuous tuning to achieve efficient irradiation in a resonant microwave source

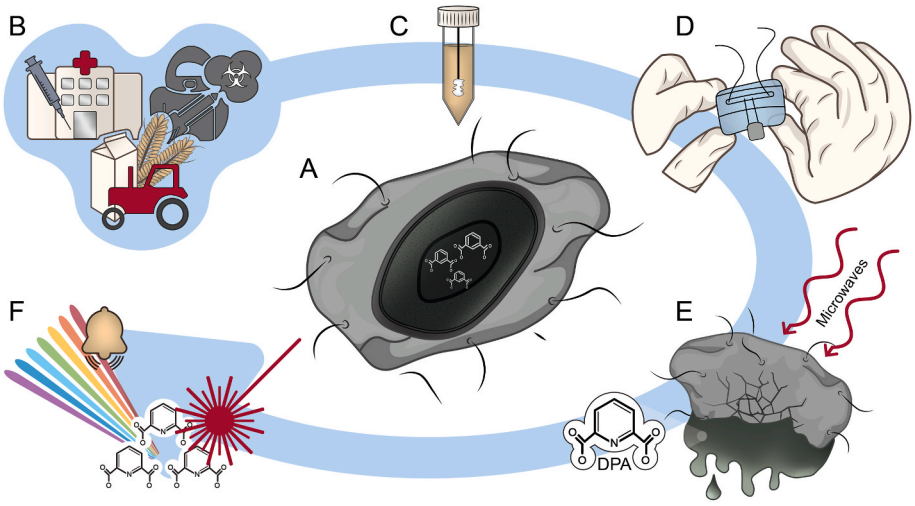

Fig. 1. Schematic illustration of the microwave induced spore breakdown and biosensing process. Pathogenic bacterial endospores contain high amounts of CaDPA in their core (A). These spores are a hazard in several areas of society, such as in hospitals, agriculture and bioterrorism (B). Spore detection from the environment is a challenge due to the resilient character of the spores. Here we show a technique for detecting spores from a sample (C) by using a waveguide-based lab-on-a-chip (D). By applying microwaves, the protective layers of the spores are disrupted and CaDPA leaks out from the spore core into a buffer (E). The CaDPA can then be detected by various spectroscopic techniques, such as fluorescence and Raman spectroscopy (F).

(Pozar, 2011).

In our experiments, we instead use a short section non-resonant CPW for a microwave applicator, as this does not need to be tuned and has much greater manufacturing tolerances. The narrow gap between the conductors still results in a high applied electric field on the sample for a given input power, comparable to that achieved in high Q resonant microwave applicators. Our CPW is based on a design by Williams et al. (2018) and can easily be made on a dual-layer PCB. The PCB is made from a 1.27 mm thick dielectric laminate (TMM10, Rogers Corporation) with relative permittivity 9.20 ± 0.23, covered on both sides with a 17.5 μm thick copper layer. The CPW applicator consists of a copper strip, 3 mm wide and 20 mm long, that is separated from the surrounding ground plane by a 1 mm gap. The applicator is connected to the RF power source by a soldered SMA connector (RS PRO 50 Ω, RS) and the ground plane is connected to the RF source ground, along with the whole bottom layer. We connected a microwave signal generator (SG4400L, DS Instruments) to the CPW through a +21 dB power amplifier (ZX60-P103LN, Mini-Circuits), and the signal generator was controlled by computer software (Signal Generator Control Pro V5.69, DS Instruments).

To make the device, we milled a gap into the copper layer and drilled two holes (1 mm in diameter) on the applicator ends. The holes are intended to allow for observational optical microscopy and visual tracking of the spores. However, we did not use these in this study and therefore covered them with tape from underneath. The CPW is designed to have a characteristic impedance Z_0 of 50 Ω at 2.45 GHz. It is thereby impedance matched to the other microwave circuitry, resulting in minimal interface reflections and losses. On the contrary, there is total reflection at the end of the CPW applicator, where the sample channel is located. This means that the voltage amplitude there is double that of the incident microwave signal, i.e.,

$$V_0 = 2\sqrt{2P_0Z_0}, \quad (1)$$

where P_0 is the rms microwave input power. This gives ~20 V per 1 W of incident power between the open circuit end of the copper strip and the adjacent ground plane. The electric field is highly non-uniform in the CPW gap and peaks at the conductor edges. Nevertheless, we can estimate the magnitude of the applied electric field near the centre of the gap as $E_0 \approx V/S$, where the gap width is $S = 1$ mm for our applicators. This yields an applied electric field of $E_0 \approx 20$ kV/m per 1 W of input power. A spore sample will thereby be exposed to this high electric field region for all microwave frequencies of interest. Further, the microwave effect on the spore is driven by the square of the electric field density (i.e., doubling the field gives 4 times the effect), whether through heating or purely electromagnetic. Thus, the high field strength for such low input power is an advantage of this system. However, without a detailed model of both spore geometry and dielectric properties of each internal layer within a spore, it is impossible to map out the internal electric field within the spore. As such, we use the applied field as a means of quantifying the microwave action.

2.2. Construction, simulation, and characterization of the microfluidic system

Our lab-on-a-chip device is built around the CPW as described in the previous section. We then added a 1 mm wide and 10 mm long microfluidic channel at the end of the CPW applicator, as seen in Fig. 2A. The channel walls were made from Parafilm M (P 7793, Sigma-Aldrich, Inc), resulting in a channel height of 130 μm. A template designed in Inkscape (v1.2, Inkscape Project) was used to cut the channel outline under an optical microscope. For the channel roof, we cut a 1 mm thick glass slide (no 1, Paul Marienfeld GmbH & Co) to a size of 25 × 15 mm and drilled two holes (1 mm in diameter) to serve as in- and outlets. We then bonded it to the Parafilm layer by heating them together on a hotplate for 2 min at 50 °C, after which we bonded the channel to the circuit by heating the two on a hotplate for 5 min at 50 °C. To introduce fluid into the device, we made hose connectors from 3 mm high PDMS cylinders (8 mm diameter). These cylinders were center punched with a biopsy punch (49101, Kai Industries & Co.) to accept 10 mm long glass capillary tubes (0820.1, Carl Roth) and mounted directly above the in and outlet holes in the glass slide. We improved the seal along the channel by adding uncured PDMS (Sylgard 184, Dow Corning) along the seams of the connectors and where the central trace meets the Parafilm, followed by curing on a hotplate for 1 h at 50 °C. Lastly, the inlet was connected to a syringe pump (VIT-FIT, Lambda Instruments), set to inject the spore suspension at a flow speed of 0.2 mm/s, through the channel. Manufacturing the chip takes less than 2h in labor time and $15 in material cost. The fabricated chip can be seen in Fig. 2B, in which the channel is filled with a blue-colored buffer.

To model the electric field generated by our lab-on-a-chip device, we used finite element simulations in COMSOL Multiphysics (v6.0, COMSOL AB) with the electromagnetic waves module. This allowed us to study the intensity distribution of the electric field and determine the amount of radiation in the microfluidic channel. The interaction with the channel was improved using a heat transfer and a laminar flow module to recreate the experimental conditions. Since electric fields also generate heat, we tracked the temperature of the sample fluid during microwave exposure to make sure that there is no significant thermal effect on the spores. First, we used a thermal camera (AX5, Teledyne FLIR LLC) and recorded the data using ResearchIR MAX (4.40, Teledyne FLIR LLC) software. To improve transmission and avoid reflections from the glass slide, we replaced it with a 13 μm thick plastic film. The modified device is shown in Fig. S1A, along with a measurement ROI placed in the center of the channel. Second, we compared this measurement with our simulation by calculating the temperature in the

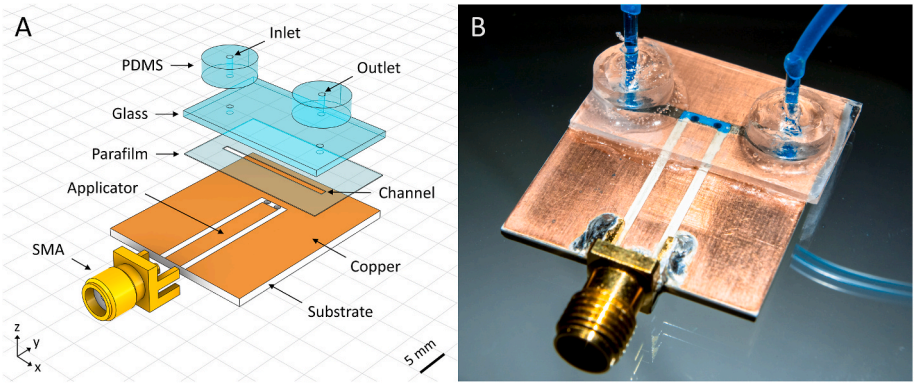

Fig. 2. The microwave microfluidic device for disrupting spores used in this study is based on a coplanar waveguide (CPW) and microfluidic channel. Panel A shows an exploded diagram of all the components that makes up the device. Panel B shows the finished device with the channel filled with a blue-colored buffer.

center of the channel as a function of time and until steady state was reached, as shown in Fig. S2A.

2.3. Spore preparation

We used *Bacillus thuringiensis* ATCC 35646 cells grown on BBLK agar (210912, BD) plates and set to incubate at 30 °C overnight. These cells were collected by scraping them off the agar and transferring them to a 1.5 ml Eppendorf tube, after which they were centrifuged to remove leftover growth media. To allow sporulation, we then stored the cells at 4 °C overnight. Before use, the sporulated suspension was rinsed five times by centrifuging in deionised water for 5 minutes at 5000 *G*. The spore samples were finally made to a concentration of 10^7 spores/ml before being introduced into the microwave chip.

2.4. Fluorescence spectroscopy

We measured fluorescence on bulk spore samples using a fluorescence spectrophotometer (Cary Eclipse, Agilent). First, the spores were dispersed in water at a concentration of 10^6 spores/ml. To confirm that an appropriate optical density for fluorescence measurements, we used a UV–Vis spectrophotometer (Lambda 650, PerkinElmer). During fluorescence measurements, we measured excitation-emission maps (EEM) displaying the fluorescence emission between 230 and 800 nm for excitations between 220 and 500 nm (in steps of 10 nm). All spectra were corrected for the wavelength-dependent optical properties of the fluorescence spectrophotometer.

2.5. Raman spectroscopy

To perform Raman spectroscopy, we used our LTRS instrument which is based on an inverted microscope (IX 71, Olympus) (Stangner et al., 2018; Dahlberg et al., 2020). This system produces an optical trap that can trap, move, and acquire Raman spectra on single spores in a sample liquid. In the lower expansion port of the microscope, we introduce a Gaussian laser beam at a wavelength of 785 nm (08-NLD, Cobolt AB) using a dichroic shortpass mirror with a 650 nm cut-off (DMSP650, Thorlabs). We image a sample and focus the laser beam using a 60× water immersion objective (UPlanSApo60xWIR, Olympus) with a numerical aperture of 1.2 and a working distance of 0.28 mm. Backscattered light from the spore samples is collected by the microscope objective and passed through a 808 nm notch filter (NF808-34, Thorlabs) to block the Rayleigh scattered light and only let the Raman signal through. To increase the signal-to-noise ratio further, we place a 150 μm diameter pinhole in the focal point of the telescope. Finally, we couple the filtered light into our spectrometer (Model 207, McPherson) through a 150 μm wide entrance slit. Inside the spectrometer, a 600 grooves/mm holographic grating with an 800 nm blaze wavelength disperses the light onto a Peltier cooled CCD detector (Newton 920 N-BR-DDXW-RECR, Andor) operated at −95 °C. To control the detector and acquire Raman spectra, we use Solis (Solis v4.30, Andor) software. This allows us to measure the Raman signal with a spectral resolution of less than 3 cm^{-1}.

To prepare a sample for Raman spectroscopy, we used a 0.15 mm thick 24 × 60 mm glass coverslip (no 1, Paul Marienfeld GmbH & Co). On this, we placed a grease ring (High vacuum grease, Dow Corning), roughly 1 cm in diameter and 1 mm in thickness. Inside the ring, we placed 10 μl of the spore suspension and then sealed it from above using a 0.15 mm thick 23 × 23 mm coverslip (no 1, Paul Marienfeld GmbH & Co). The sample was then placed in the LTRS instrument, where spores can be trapped and characterized based on their biochemical content. To minimise the background Raman signal from the glass, we moved the spores 50 μm above the glass surface before measurements. When measuring Raman spectra, we used ~60 mW laser power (in the sample) and performed 2 accumulations of 10 s each. This dose of 785 nm light is significantly lower than what is harmful to spores and does not disrupt the spore bodies (Malyshev et al., 2022d, 2022b). We measured at least 100 individual spores for each experimental set.

2.6. SEM imaging

To prepare a sample for SEM imaging, we air dried a 3 μL drop of spore suspension on a glass slide and coated the sample with a 5 nm thick layer of platinum using a sputter coater (Q150T-ES, Quorum Technologies Ltd). We imaged the spores using a scanning electron microscope (Merlin FESEM, Carl Zeiss), using its InLens imaging mode at a magnification of 15000-50000×.

2.7. Data analysis

To baseline correct our Raman spectra, we used an asymmetrical least-squares algorithm (Eilers, 2004) with $\lambda = 10^5$ and $p = 10^{-3}$. We smoothed the spectra using a first-degree Savitzky-Golay filter (frame length of 5). These functions are part of an open-source Matlab program provided by the Vibrational Spectroscopy Core Facility (VISP). To see how the peak intensities changed over time, we normalized the spectra with respect to their initial values, with the differences in the proportions of spores containing the CaDPA peak calculated using the Chi-squared test. To perform statistical analysis of differences in the CaDPA peak intensities, we used Prism (Prism 9.3, GraphPad Software) and a one-way ANOVA with the Kruskal–Wallis test for multiple comparisons. In Prism, we also performed principal component analysis (PCA) of the whole Raman spectra. All data used in the PCA is mean-centered, with the PCA based on the data correlation matrix, and the graphs were plotted in Origin 2018 (OriginLab).

2.8. Spore CaDPA content quantification

To determine the amount of spore CaDPA content, we used baseline-corrected spectra and checked for the presence of a 1017 CaDPA cm^{-1} peak. We determined peak prominence by identifying local maxima in the 1010–1020 cm^{-1} range and compared it to the CaDPA peak in the control sample (untreated spores). If a peak had an intensity of >10% of the median value in the control, the spores were considered to contain CaDPA, while those with less were not. We observed a bimodal distribution of peak prominence in the experimental data, and with our method, there were no spectra where the presence of CaDPA was unclear. Similarly, we identified non-spore debris by checking for the absence of the 1001 cm^{-1} phenylalanine peak in the spectra.

2.9. DNA content evaluation

To determine if DNA was released from the spores, we used a Bioanalyzer fluorescence electrophoresis system (2100 Bioanalyzer Instrument, Agilent Technologies, Inc.). The supernatants of the spore suspensions of the microwaved and control sample were evaluated using the high sensitivity DNA assay.

3. Results and discussion

3.1. Simulated electrical field distribution and generation of heat

To generate a localised microwave field strong enough to disrupt spores, we used a CPW applicator design by Williams et al. (2018). However, since we added a microfluidic channel in our design, which may influence the electric field distribution, we modeled the complete device in COMSOL Multiphysics to characterize the electric field in the channel, see Fig. 3. The material properties used in our simulations are summarized in Table 1. We found that the electric field reaches a value of $> 1.8 \cdot 10^4$ V/m, peaking at the conductor edges, which is in line with theoretical predictions. Where the channel passes the applicator, the electric field in the sample is mostly uniform and with a strength of 1.2 ·

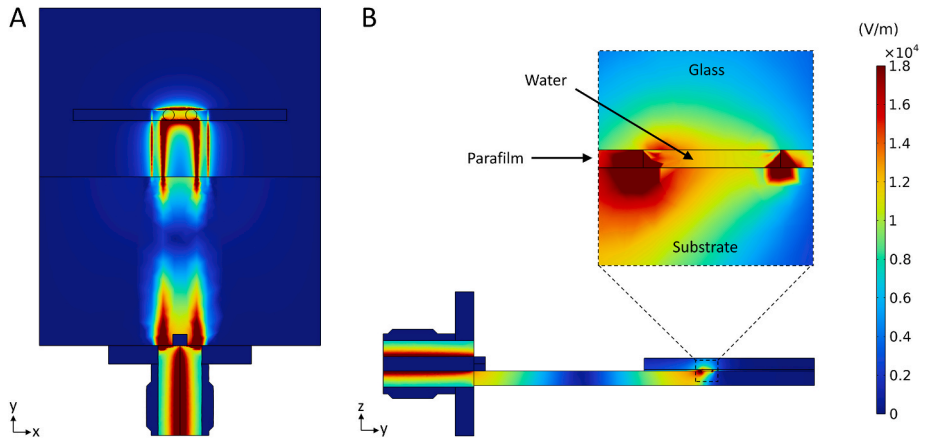

Fig. 3. Simulated electric field distribution for the CPW device. Panel A shows the electric field norm at the top surface of the PCB, which is the bottom of the microfluidic channel. Panel B shows the electric field norm at a cut plane through the center of the device, with an inset focused around the channel that contains the spore suspension. The PCB substrate have a thin layer of copper on the top and the bottom surface, with the CPW cut into it (not visible here).

Table 1
Summary of material properties of the channel used in the COMSOL simulation. The temperature dependent loss factor (complex permittivity) for water, $\varepsilon''_w(T)$, is an important property for microwave heating and it has been interpolated from tabulated imperial data, as seen in Fig. S2B. Other values are specified at room temperature (297 K).

Property	Water (Milli-Q)	Parafilm (Polyethylene)	Glass (Quartz)	Copper (Pure)	Substrate (TMM10)
Thermal conductivity (W/(m·K))	5.98e-1	3.8e-1	1.4	4.0e2	7.6e-1
Electrical conductivity (S/m)	2.0e-3	1.0e-12	1.0e-14	6.0e7	5.0e-13
Relative permittivity	8.0e1 - $\varepsilon''_w \cdot i$	2.3–3.0e-4 · i	4.2	1	9.2
Relative permeability	1	1	1	1	1
Dynamic viscosity (Pa·s)	1e-3	–	–	–	–
Density (kg/m^3)	9.97e2	9.3e2	2.21e3	8.96e3	2.77e3
Heat capacity (J/(kg·K))	4.19e3	1.9e3	7.3e2	3.85e2	7.4e3

10^4 V/m. Outside of this area, the electric field falls off rapidly making it safe to handle and operate, as seen in Fig. S3. The results from our simulation also show an electric field hotspot close to the SMA connector, not present in previous simulations on this CPW (Williams et al., 2018). This hotspot is due to our channel giving rise to a slight change in the impedance of the CPW. Without the channel, the electric fields are identical to previous studies.

Electric field hotspots will also give rise to heat in the channel. Using a thermal camera, we measured a temperature increase of ~0.5 °C in the center of the channel at 1.2 W of input power, see Fig. S1B. This can be compared with the simulation, where we found a ~4 °C temperature increase in the center of the channel, as seen in Figs. S2A and S4. The disparity in temperature is likely caused by us removing the thick insulating glass slide before measuring with the thermal camera. However, this heating is still significantly lower than that of a commercial microwave oven while providing the same field strength. Although there is a possibility of localised hotspots within each spore, owing to their inhomogeneous geometry and dielectric properties (Malyshev et al., 2019), it is unlikely to cause thermal disruption since spores are capable of withstanding temperatures exceeding 100 °C (Setlow, 2006). We therefore conclude that any effects on the spores from our treatment are likely non-thermal in nature.

3.2. Microwave electric field disrupts spores

We then expose spores to a 2.45 GHz microwave field in the CPW. We used input powers of 5 dBm and 10 dBm from the microwave source which, combined with the 21 dB power amplifier, resulted in input powers of 0.4 W (26 dBm) and 1.2 W (31 dBm), respectively. The spore suspension passes through the channel with an average flow velocity of 0.2 mm/s in all experiments, implying that spores in the channel are exposed to the electric field for approximately 15 s. After exposure to the microwave field, the suspensions were collected in 1.5 ml Eppendorf tubes at a rate of 94 μl/h. We also pass suspensions through the microfluidic channel without any power input (0 W) as a control. We then characterized the chemical changes of the spore suspensions in bulk using fluorescence spectroscopy and in individual spores using LTRS.

3.2.1. Fluorescence spectroscopy indicates breakdown of spore protein structure

Fluorescence spectroscopy can be used to monitor the level of certain fluorescent molecules in a solution. Within bacterial spores there are two prevalent fluorescence peaks at $\lambda_{exc/em} = 230/330$ nm and 280/330 nm, both indicating the presence of amino acids tryptophan and tyrosine (Kunnil et al., 2005; Yang et al., 2017). In addition to tryptophan and tyrosine, the amino acid phenylalanine is also known to fluoresce in the nearby regions $\lambda_{exc/em} = 210/280$ nm and 260/280 nm. However, due to its relatively low quantum yield compared to tryptophan and tyrosine, this fluorescence signal is often masked (Yang et al., 2017). As such, phenylalanine is more readily measured in spores using Raman spectroscopy where it displays a prominent characteristic peak (Esposito et al., 2003; De Gelder et al., 2007). These amino acids are central in constructing proteins vital to the spore, making up among other things the coat layer that encloses and protects the spore genetic material (Stewart, 2015). Fluorescence can also be used to detect DNA in solution, using dyes like SYTO16. However, we were not able to detect DNA release in our experimental data using fluorescence (Fig. S5). Another fluorescent molecule present in spores is CaDPA. CaDPA released from the spores is known to lose its Ca-chelate and degrade into regular dipicolinic acid (DPA). In this form, DPA has been reported to fluoresce at $\lambda_{exc/em} = 330/410$ nm after exposure to UV-radiation (Nudelman et al., 2000; Johansson et al., 2022). An advantage of detecting CaDPA is that it is a small molecule that is abundant in the spore core, and the spore can naturally release it quickly.

To track changes in the proteinaceous spore coat and CaDPA, we utilize fluorescence spectroscopy. However, to verify that our samples

have an appropriate level of absorbance ahead of measuring fluorescence, we used absorbance spectroscopy. More specifically, we wanted to see that the absorbance level is sufficiently high to yield fluorescence but not too high to yield inner filter effects. We observed the absorbance from our samples with appropriate absorbance values around 0.02 at 280 nm for both control and microwave exposed samples, enough to observe fluorescence, but significantly lower than the 0.1–0.2 commonly considered maximum for fluorescence measurements. We then recorded fluorescence EEM of spore suspensions (n = 3) before and after exposure to 1.2 W microwave radiation. Before exposure, we observe clear fluorescence peaks in our EEM at $\lambda_{exc/em}$ = 230/330 and 280/330 nm (Fig. 4A), indicating the presence of tryptophan and tyrosine. However, after exposure, we find these peaks have decreased in intensity by 60–70% (Fig. 4B), indicating a change in the protein structures containing these two amino acids. Such a change may indicate a disruption in the proteinaceous spore coat containing the spore core enclosing the spore DNA and CaDPA. However, the fluorescence measurements did not indicate additional fluorescence peaks in the EEM related to any leaked out DPA content. In that regard, we cannot use this information to indicate whether the CaDPA still remains within the spore core after microwave treatment, as it is not known whether microwave exposure has the same fluorescence-enhancing effect on DPA as UV-radiation (Sarasanandarajah et al., 2005). Based on this conclusion, we apply LTRS to study, at the single spore level, if CaDPA was released from the spores after microwave treatment.

3.2.2. LTRS and SEM indicate spore CaDPA release after microwave exposure

CaDPA is abundant in the spore core, making up to 20% of the core dry weight. It also has a strong characteristic Raman intensity peak at 1017 cm^{-1} (Setlow et al., 2006). CaDPA is released from spores during germination, but also as a result of damage to the spores' structural integrity (Zhang et al., 2019). As such, when environmental conditions are unsuitable for germination, CaDPA can be used as a natural biomarker for spore core integrity (Shibata et al., 1986; Kočišová and Procházka, 2018). We assessed the spore core integrity of spores exposed to microwave using our LTRS system, in which we trapped single spores and measured Raman spectra within the 600–1400 cm^{-1} range. In total, we measured on 3 separate samples (biological replicates) and at least 100 individual spores (technical replicates), n = 110 (0 W), n = 113 (0.4 W) and n = 135 (1.2 W).

We measured Raman signals from the spore samples, microwaved at 1.2 W, 0.4 W, and unexposed controls. The resulting spectra can be clustered into 3 separate groups with representative spectra shown in Fig. 5A. Group 1 shows spectra similar to those described in previous literature on spores, with distinct peaks at 660, 825, 1001, 1017 and 1395 cm^{-1} (Kong et al., 2012; Wang et al., 2015a; Malyshev et al., 2022a). The main component of this spectra is CaDPA from the spore core, accounting for all of the above mentioned peaks except for the 1001 cm^{-1} peak caused by phenylalanine in the spores' protein structures (Zhang et al., 2010). In group 2, only the 1001 cm^{-1} phenylalanine peak is present, although with its intensity decreased by approximately 70% compared to untreated spores. This decrease is in line with previous fluorescence measurements showing a decrease in the amino acid signal by 60–70%, further suggesting a breakdown in the spore protein structure. Overall, the lack of CaDPA-related peaks, alongside the decrease in the amino acid related peak at 1001 cm^{-1}, indicates the breakdown of the spore and subsequent release of CaDPA. Group 3 is the least commonly observed group, showing none of the spore-associated peaks. With just 6 acquired spectra across all measurements, it is likely from protein debris. The distribution of spore Raman spectra for different levels of microwave exposure can be seen in Table 2.

We then quantified the effect of the electric field power on the percentage of spores that have CaDPA in the core. In the untreated control, 71% of the trapped spores have a CaDPA peak. This number decreases to 52% in the 0.4 W microwave-treated spores, and further to 22% in spores treated with 1.2 W. This is a significant difference ($p < 0.0001$) and indicates that CaDPA is released as a result of the microwave exposure. The distribution of the CaDPA peak intensity in the samples can be seen in Fig. 5B, and shows the decrease in the prevalence of CaDPA in the spores with increased microwave exposure. Furthermore, the release of CaDPA from the spore during microwave treatment is further suggested using SEM imaging. Untreated spores remain largely intact, while the microwaved (1.2 W) spores appear deflated, indicating a leak in core CaDPA content, as seen in Fig. 6 and Fig. S6.

We then assessed the differences in the spores' Raman spectra using PCA, comparing all the acquired spectra (n = 358). We compared spectra by looking at the grouping of the spectra on a PCA plot, shown in Fig. 5C. We found the spectra to fall into groups corresponding to the spectra in Fig. 4A, with microwave treated spores predominantly lacking CaDPA. Overall, the differences in the CaDPA content of the spores and their morphological changes on the spores as shown through SEM shows there is a power-dependent effect on the spores from the waveguide, with microwaved spores being disrupted and releasing CaDPA.

3.3. The next steps - detecting spores using traditional and light-based methods

Our study shows that spore disruption can be achieved on small sample volumes using a compact and low-power operating device. This device can be used in the process of detecting spores, by disrupting a collected field sample and releasing the content of the spores' core. For low-concentration samples, a concentrator may be employed before disruption to improve the throughput. The next step is to detect the material that is released from the disrupted spores with high sensitivity and speed. Conventional biological methods for detection focus on the

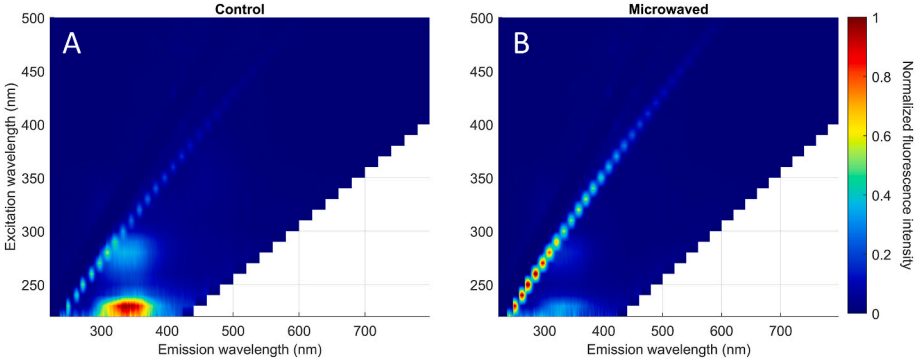

Fig. 4. EEM showing the fluorescence profile of untreated *B. thuringiensis* spores compared to their microwave exposed counterpart. Untreated spores (A) show significant fluorescence at $\lambda_{exc/em}$ = 230/330 and 280/330 nm, corresponding to e.g., amino acids tryptophan and tyrosine. These peaks are diminished by 60–70% in the microwave-treated (B) spore sample.

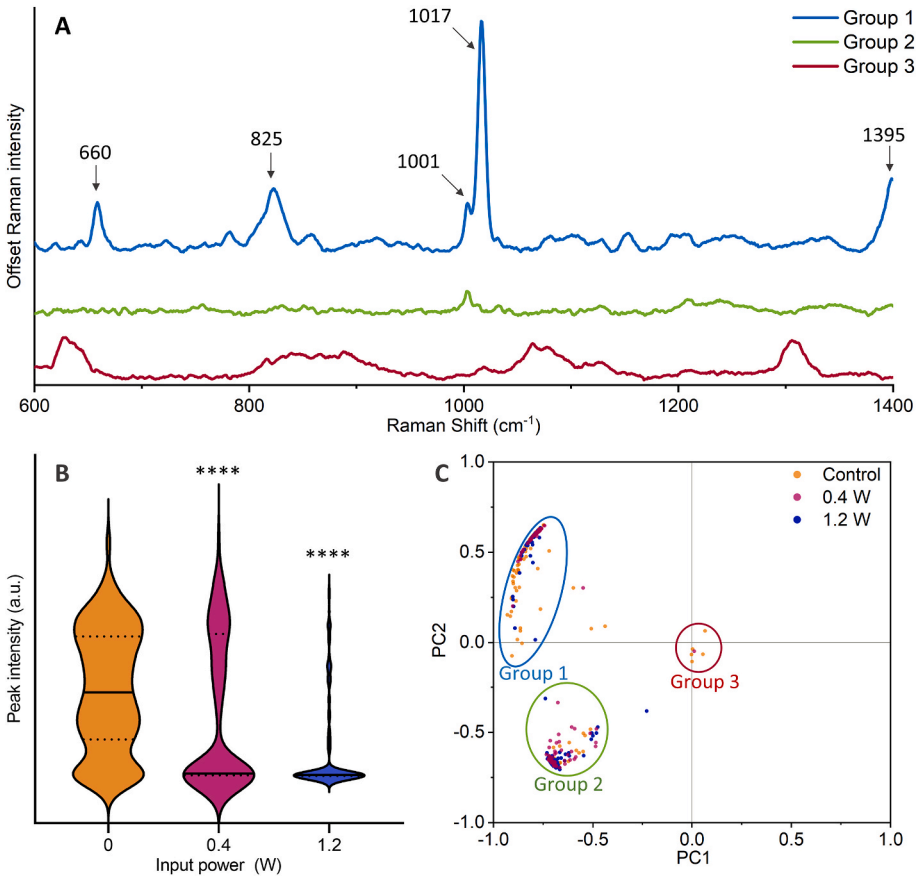

Fig. 5. Panel A shows representative spectra from the three groups of spores identified, with characteristic peaks highlighted. Panel B shows the intensity distribution of the CaDPA (1017 cm^{-1}) peaks for spores treated at 0 W, 0.4 W and 1.2 W. Solid lines show the median and the dotted line show the upper an lower quartile in the distribution. A significant number ($p < 0.0001$) of the spores microwaved at 0.4 and 1.2 W have lost their CaDPA, as compared to the control (0 W). Panel C shows the principal component analysis (PCA) of all spores and these spectra clusters were used to identify the three groups in panel A.

Table 2
Number of Raman spectra categorized as spores containing CaDPA, not containing CaDPA, and debris after exposure to microwave powers 0 W, 0.4 W, and 1.2 W respectively.

Input power (W)	CaDPA peak	No CaDPA peak	Debris
0	75	30	5
0.4	58	54	1
1.2	30	105	0

protein and DNA released by the spores utilizing antibodies and PCR, while emerging methods use nanoparticles and fluorescent hybridisation probes (Belgrader et al., 1999; Aslan et al., 2008; Joshi et al., 2014). The limitation of these methods is the lack of field-testing capability. To complement these limitations, there exists several spectroscopy-based methods that provide the ability to rapidly detect spore biomarkers on the go.

Raman spectroscopy, as used in this study, is a well explored method for spore detection and identification. Indeed, it is even able to identify spores on a species level as long as sufficiently detailed spectral libraries have been pre-built (Stockel et al., 2012). These studies are often performed only on intact spores, meaning the libraries cannot be used for disrupted spores. However, with expanded libraries and development of new and more robust machine learning classification algorithms it might be possible to apply these to identify spores on a species level in the future. Furthermore, the inherent low sensitivity of Raman scattering

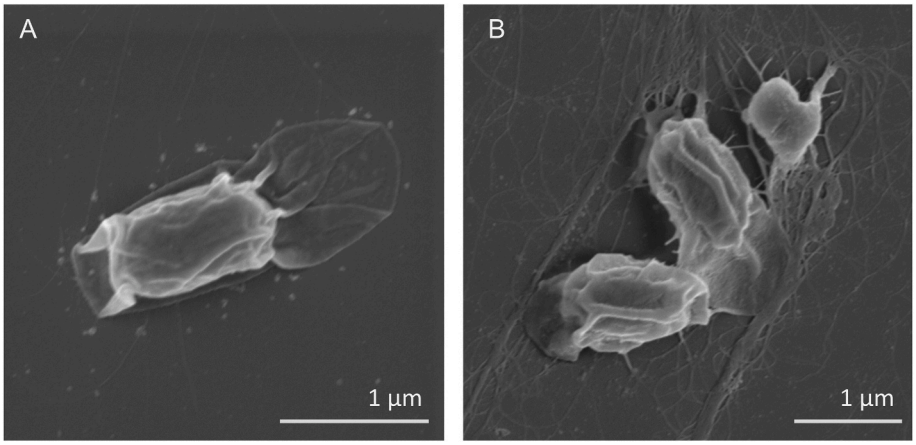

Fig. 6. SEM micrographs of *B. thuringiensis* spores. Untreated spores (A) are visually intact, as expected, while spores subjected to a 1.2W appear collapsed (B).

makes it challenging to detect low quantities of spores, whether disrupted or healthy. One method to improve the sensitivity of Raman is through SERS. By utilizing surface plasmon effects on nanostructured metal surfaces, Raman signals can be enhanced by factors upward of 10^{10}. However, this enhancement is very local to the metal surface. As such internal biomarkers like CaDPA, which reside deeper within the spore structure, are not significantly enhanced in intact spores. By disrupting the spore and releasing the CaDPA, it is possible to detect the CaDPA using SERS (Farquharson et al., 2004). Despite these advantages, SERS still has shortfalls like limited Raman signal reproducibility between substrates and high signal noise from background contaminants. As such, SERS-based detection assays should be performed with caution for now. However, with better reproducibility between substrates and robust techniques to remove background contaminants, identification of CaDPA using SERS can be a suitable detection method in future devices.

Fluorescence is also a widely studied method for spore detection, with spore autofluorescence being a common method for determining spore viability (Laflamme et al., 2005; Johansson et al., 2022). However, the fluorescence signal from spores is non-specific, with CaDPA exhibiting a low fluorescence yield and other fluorescent species being common to other pathogenic and non-pathogenic bacteria. As such spore autofluorescence is a poor method for specific spore detection. To improve upon the specificity of spore detection through fluorescence, there exist several methods for boosting the fluorescence signal of the CaDPA and one of these is UV-exposure. By exposing the non-chelated form of CaDPA (DPA) to UV-radiation, the molecule dimerizes, as shown by Nardi et al. (2021). This correlates with an increase in fluorescence yield around $\lambda_{exc/em} = 320/410$ nm (Sarasanandarajah et al., 2005), allowing for the detection of a spore-specific fluorescence signal. However, these studies have so far focused on pure DPA solutions, and as such, the method's applicability to real spore samples is largely unexplored. Another method to improve the fluorescence signal of DPA is by adding terbium ions. Terbium ions exhibit a fluorescence pattern when exposed to light at 270 nm. The fluorescence yield of this pattern is then greatly enhanced when terbium is allowed to mix and chelate with DPA, creating an effective fluorescent biomarker (Pellegrino et al., 1998). This method for spore detection has been well-explored, with several studies which further develop the detection protocol using various nanostructure approaches (Bhardwaj et al., 2016; Liu et al., 2019). Terbium enhanced fluorescence suffers from similar downsides as SERS, with the DPA having to be released from the spore core to be able to form a chelate with the terbium. With proper spore disruption, it may be a useful technique for spore detection. Thus, overall there exist many light-based methods to detect spores, both whole and disrupted. However, the most sensitive techniques benefit from spore disruption, releasing the spore-specific biomarkers for signal enhancement and detection.

In conclusion, this project marks an important step towards developing a lab-on-a-chip device for small-scale biosensing applications related to spore detection. The future directions of this research program will focus on enhancing the sensor's sensitivity and selectivity, with the ultimate goal of exploring its use in point-of-care testing similar to other lab-on-chip devices in development (Vashist et al., 2015). Moreover, we anticipate that the technique can be extended to food safety testing, where it could identify specific biomarkers indicating the presence of contaminants.

4. Conclusions

Bacterial spores are resilient forms of bacteria, capable of causing great damage within the food industry and civil society. One prevalent and specific biomarker for detecting spores is CaDPA, which is sealed off within the spore core by a protective protein coat. Here we have shown that using a lab-on-a-chip containing a coplanar waveguide (CPW) applicator, it is possible to disrupt the spore coat and release the CaDPA biomarker from spores, for detection with fluorescence. The release of CaDPA is a result of the high electric field in the microfluidic channel, generated across the narrow gap at the end of the CPW applicator. When microwaving spore samples at 1.2 W of input power ($\sim 1.2{\cdot}10^4$ V/m), we find a 70% decrease in fluorescence associated with key amino acids. Evaluating individual spores from the same treatment, we find that microwave radiation induces CaDPA release in more than 75% of the spores. Overall, this study highlights the use of a portable CPW for disrupting spores, allowing for easier detection of spore biomarker.

CRediT authorship contribution statement

Shayan Valijam: Investigation, (Waveguide, Raman), Software, (COMSOL Model), Formal analysis, Writing – original draft. **Daniel P.G. Nilsson:** Investigation, (Waveguide, thermal), Software, (COMSOL Model, Formal analysis, Writing – review & editing. **Rasmus Öberg:** Investigation, (Fluorescence), Formal analysis, Writing – review & editing. **Unni Lise Albertsdóttir Jonsmoen:** Visualization, Writing – review & editing. **Adrian Porch:** Validation, (Waveguide), Formal analysis, (Waveguide), Writing – review & editing. **Magnus Andersson:** Supervision, Project administration, Funding acquisition, Resources, Writing – review & editing. **Dmitry Malyshev:** Conceptualization, Methodology, Supervision, Formal analysis, Writing – original draft, Writing – review & editing.

Declaration of competing interest

The authors declare that they have no known competing financial interests or personal relationships that could have appeared to influence the work reported in this paper.

Data availability

Data will be made available on request.

Acknowledgement

This work was supported by the Swedish Research Council (2019–04016); the Swedish Foundation for Strategic Research; the Umeå University Industrial Doctoral School (IDS); Kempestiftelserna (JCK-1916.2); Swedish Department of Defence, Project no. 470-A400821, and the Norwegian University of Life Sciences (NMBUs) research fund.

The authors acknowledge the facilities and technical assistance of the Umeå Core Facility for Electron Microscopy (UCEM) at the Chemical Biological Centre (KBC), Umeå University, a part of the National Microscopy Infrastructure NMI (VR-RFI 2016-00968). We thank Anna-Lena Johansson at FOI for providing the original stock of spores for this project.

Appendix A. Supplementary data

Supplementary data to this article can be found online at https://doi.org/10.1016/j.bios.2023.115284.

References

Abduljabar, A.A., Clark, N., Lees, J., Porch, A., 2017. Dual mode microwave microfluidic sensor for temperature variant liquid characterization. IEEE Trans. Microw. Theor. Tech. 65, 2572–2582. https://doi.org/10.1109/TMTT.2016.2647249.

Andersson, A., Ronner, U., Granum, P.E., 1998. What problems does the food industry have with the spore-forming pathogens Bacillus cereus and Clostridium perfringens? Doktorsavhandlingar Vid. Chalmers Tek. Hogskola 28, 145–155.

Aslan, K., Previte, M.J.R., Zhang, Y., Gallagher, T., Baillie, L., Geddes, C.D., 2008. Extraction and detection of DNA from Bacillus anthracis spores and the vegetative cells within 1 min. Anal. Chem. 80, 4125–4132. https://doi.org/10.1021/ac800519r.

Belgrader, P., Hansford, D., Kovacs, G.T.A., Venkateswaran, K., Mariella, R., Milanovich, F., Nasarabadi, S., Okuzumi, M., Pourahmadi, F., Northrup, M.A., 1999.

A minisonicator to rapidly disrupt bacterial spores for DNA analysis. Anal. Chem. 71, 4232–4236. https://doi.org/10.1021/ac990347o.
Bhardwaj, N., Bhardwaj, S., Mehta, J., Kim, K.H., Deep, A., 2016. Highly sensitive detection of dipicolinic acid with a water-dispersible terbium-metal organic framework. Biosens. Bioelectron. 86, 799–804.
Celandroni, F., Longo, I., Tosoratti, N., Giannessi, F., Ghelardi, E., Salvetti, S., Baggiani, A., Senesi, S., 2004. Effect of microwave radiation on Bacillus subtilis spores. J. Appl. Microbiol. 97, 1220–1227. https://doi.org/10.1111/j.1365-2672.2004.02406.x.
Dahlberg, T., Malyshev, D., Andersson, P.O., Andersson, M., 2020. Biophysical fingerprinting of single bacterial spores using laser Raman optical tweezers. In: Guicheteau, J.A., Howle, C.R. (Eds.), Chemical, Biological, Radiological, Nuclear, and Explosives (CBRNE) Sensing XXI. SPIE, p. 28. https://doi.org/10.1117/12.2558102.
de Bruin, O.M., Chiefari, A., Wroblewski, D., Egan, C., Kelly-Cirino, C.D., 2019. A novel chemical lysis method for maximum release of DNA from difficult-to-lyse bacteria. Microb. Pathog. 126, 292–297. https://doi.org/10.1016/j.micpath.2018.11.008.
De Gelder, J., Scheldeman, P., Leus, K., Heyndrickx, M., Vandenabeele, P., Moens, L., De Vos, P., 2007. Raman spectroscopic study of bacterial endospores. Anal. Bioanal. Chem. 389, 2143–2151. https://doi.org/10.1007/s00216-007-1616-1.
Eilers, P.H.C., 2004. Parametric time warping. Anal. Chem. 76, 404–411. https://doi.org/10.1021/ac034800e.
Esposito, A.P., Talley, C.E., Huser, T., Hollars, C.W., Schaldach, C.M., Lane, S.M., 2003. Analysis of single bacterial spores by micro-Raman spectroscopy. Appl. Spectrosc. 57, 868–871. https://doi.org/10.1366/000370203322102979.
Farquharson, S., Gift, A., Maksymiuk, P., Inscore, F.E., Smith, W.W., 2004. pH dependence of methyl phosphonic acid, dipicolinic acid, and cyanide by surface-enhanced Raman spectroscopy. In: Sedlacek III, A.J., Colton, R., Vo-Dinh, T. (Eds.), Chemical and Biological Point Sensors for Homeland Defense, p. 117. https://doi.org/10.1117/12.510626.
Goel, A.K., 2015. Anthrax: a disease of biowarfare and public health importance. World J. Clin. Cases. 3, 20. https://doi.org/10.12998/wjcc.v3.i1.20.
Johansson, A.C., Landström, L., Öberg, R., Andersson, P.O., 2022. Monitoring deactivation processes of bacterial spores using fluorescence spectroscopy. In: Guicheteau, J.A., Howle, C.R. (Eds.), Chemical, Biological, Radiological, Nuclear, and Explosives (CBRNE) Sensing XXIII. SPIE, p. 32. https://doi.org/10.1117/12.2623447.
Joshi, L.T., Mali, B.L., Geddes, C.D., Baillie, L., 2014. Extraction and sensitive detection of toxins A and B from the human pathogen Clostridium difficile in 40 seconds using microwave-accelerated metal-enhanced fluorescence. PLoS One 9, 16–18. https://doi.org/10.1371/journal.pone.0104334.
Kim, S.Y., Shin, S., Song, C.H., Jo, E.K., Kim, H.J., Park, J.K., 2009. Destruction of Bacillus licheniformis spores by microwave irradiation. J. Appl. Microbiol. 106, 877–885. https://doi.org/10.1111/j.1365-2672.2008.04056.x.
Kočišová, E., Procházka, M., 2018. Drop coating deposition Raman spectroscopy of dipicolinic acid. J. Raman Spectrosc. 49, 2050–2052. https://doi.org/10.1002/jrs.5493.
Kong, L., Setlow, P., Li, Y.q., 2012. Analysis of the Raman spectra of Ca2+-dipicolinic acid alone and in the bacterial spore core in both aqueous and dehydrated environments. Analyst 137, 3683. https://doi.org/10.1039/c2an35468c.
Kunnil, J., Sarasanandarajah, S., Chacko, E., Reinisch, L., 2005. Fluorescence quantum efficiency of dry *Bacillus globigii* spores. Opt Express 13, 8969. https://doi.org/10.1364/OPEX.13.008969.
Laflamme, C., Verreault, D., Lavigne, S., Trudel, L., Ho, J., Duchaine, C., 2005. Autofluorescence as a viability marker for detection of bacterial spores. Front. Biosci. Landmark. 10, 1647–1653.
Li, Q., Sun, K., Chang, K., Yu, J., Chiu, D.T., Wu, C., Qin, W., 2013. Ratiometric luminescent detection of bacterial spores with terbium chelated semiconducting polymer dots. Anal. Chem. 85, 9087–9091. https://doi.org/10.1021/ac4016616.
Liu, M.L., Chen, B.B., He, J.H., Li, C.M., Li, Y.F., Huang, C.Z., 2019. Anthrax biomarker: an ultrasensitive fluorescent ratiometry of dipicolinic acid by using terbium (iii)-modified carbon dots. Talanta 191, 443–448.
Malyshev, D., Williams, C.F., Lees, J., Baillie, L., Porch, A., 2019. Model of microwave effects on bacterial spores. J. Appl. Phys. 125 https://doi.org/10.1063/1.5085442.
Malyshev, D., Dahlberg, T., Öberg, R., Landström, L., Andersson, M., 2022a. Reference Raman spectrum and mapping of *Cryptosporidium parvum* oocysts. J. Raman Spectrosc. 1–9. https://doi.org/10.1002/jrs.6361.
Malyshev, D., Öberg, R., Dahlberg, T., Wiklund, K., Landström, L., Andersson, P.O., Andersson, M., 2022b. Laser induced degradation of bacterial spores during micro-Raman spectroscopy. Spectrochim. Acta Mol. Biomol. Spectrosc. 265, 120381 https://doi.org/10.1016/j.saa.2021.120381.
Malyshev, D., Öberg, R., Landström, L., Andersson, P.O., Dahlberg, T., Andersson, M., 2022c. pH-induced changes in Raman, UV–vis absorbance, and fluorescence spectra of dipicolinic acid (DPA). Spectrochim. Acta Mol. Biomol. Spectrosc. 271, 120869 https://doi.org/10.1016/j.saa.2022.120869.
Malyshev, D., Robinson, N.F., Öberg, R., Dahlberg, T., Andersson, M., 2022d. Reactive oxygen species generated by infrared laser light in optical tweezers inhibits the germination of bacterial spores. J. Biophot. 15, 1–7. https://doi.org/10.1002/jbio.202200081.
Manchee, R.J., Broster, M.G., Anderson, I.S., Henstridge, R.M., Melling, J., 1983. Decontamination of Bacillus anthracis on gruinard island? Nature 303, 239–240. https://doi.org/10.1038/303239a0.
Monteiro, J., Costa, L.C., Valente, M.A., Santos, T., Sousa, J., 2011. Simulating the electromagnetic field in microwave ovens. SBMO/IEEE MTT-S Int. Microwave. Optoelectron. Conf. Proceed. 493–497. https://doi.org/10.1109/IMOC.2011.6169274.
Nardi, G., Lineros-Rosa, M., Palumbo, F., Miranda, M.A., Lhiaubet-Vallet, V., 2021. Spectroscopic characterization of dipicolinic acid and its photoproducts as thymine photosensitizers. Spectrochim. Acta Mol. Biomol. Spectrosc. 245, 118898 https://doi.org/10.1016/j.saa.2020.118898.
Nudelman, R., Bronk, B.V., Efrima, S., 2000. Fluorescence emission derived from dipicolinic acid, its sodium, and its calcium salts. Appl. Spectrosc. 54, 445–449. https://doi.org/10.1366/0003702001949564.
Osimani, A., Aquilanti, L., Clementi, F., 2018. *Bacillus cereus* foodborne outbreaks in mass catering. Int. J. Hospit. Manag. 72, 145–153. https://doi.org/10.1016/j.ijhm.2018.01.013.
Pellegrino, P.M., Fell, N.F., Rosen, D.L., Gillespie, J.B., 1998. Bacterial endospore detection using terbium dipicolinate photoluminescence in the presence of chemical and biological materials. In: Biomedical Optical Spectroscopy and Diagnostics/Therapeutic Laser Applications. OSA, Washington, D.C., p. PR3. https://doi.org/10.1364/BOSD.1998.PR3
Pellegrino, P.M., Fell, N.F., Gillespie, J.B., 2002. Enhanced spore detection using dipicolinate extraction techniques. Anal. Chim. Acta 455, 167–177. https://doi.org/10.1016/S0003-2670(01)01613-0.
Pozar, D.M., 2011. Microwave Engineering, fourth ed. John Wiley & sons.
Sarasanandarajah, S., Kunnil, J., Bronk, B.V., Reinisch, L., 2005. Two-dimensional multiwavelength fluorescence spectra of dipicolinic acid and calcium dipicolinate. Appl. Opt. 44, 1182–1187. https://doi.org/10.1364/AO.44.001182.
Setlow, P., 2006. Spores of *Bacillus subtilis*: their resistance to and killing by radiation, heat and chemicals. J. Appl. Microbiol. 101, 514–525. https://doi.org/10.1111/j.1365-2672.2005.02736.x.
Setlow, B., Atluri, S., Kitchel, R., Koziol-Dube, K., Setlow, P., 2006. Role of dipicolinic acid in resistance and stability of spores of Bacillus subtilis with or without DNA-protective α/β-type small acid-soluble proteins. J. Bacteriol. 188, 3740–3747. https://doi.org/10.1128/JB.00212-06.
Shibata, H., Yamashita, S., Ohe, M., Tani, I., 1986. Laser Raman spectroscopy of lyophilized bacterial spores. Microbiol. Immunol. 30, 307–313.
Simons, R.N., 2004. Coplanar Waveguide Circuits, Components, and Systems. John Wiley & Sons.
Sorrentino, R., Bianchi, G., 2010. Microwave and RF Engineering. John Wiley & Sons.
Stangner, T., Dahlberg, T., Svenmarker, P., Zakrisson, J., Wiklund, K., Oddershede, L.B., Andersson, M., 2018. Cooke–Triplet tweezers: more compact, robust, and efficient optical tweezers. Opt Lett. 43, 1990. https://doi.org/10.1364/ol.43.001990.
Stewart, G.C., 2015. The exosporium layer of bacterial spores: a connection to the environment and the infected host. Microbiol. Mol. Biol. Rev. 79, 437–457. https://doi.org/10.1128/MMBR.00050-15.
Stockel, S., Meisel, S., Elschner, M., Rosch, P., Popp, J., 2012. Raman spectroscopic detection of anthrax endospores in powder samples. Angew. Chem. Int. Ed. 51, 5339–5342. https://doi.org/10.1002/anie.201201266.
Vaid, A., Bishop, A., 1998. The destruction by microwave radiation of bacterial endospores and amplification of the released dna. J. Appl. Microbiol. 85, 115–122.
Vashist, S.K., Luppa, P.B., Yeo, L.Y., Ozcan, A., Luong, J.H., 2015. Emerging Technologies for next-generation point-of-care testing. Trends Biotechnol. 33, 692–705. https://doi.org/10.1016/j.tibtech.2015.09.001.
VISP, 2022. Vibrational Spectroscopy Core Facility. Umeå University. URL: https://www.umu.se/en/research/infrastructure/visp/downloads/. (Accessed 10 April 2022).
Wang, S., Shen, A., Setlow, P., Li, Y.Q., 2015a. Characterization of the dynamic germination of individual *Clostridium difficile* spores using Raman spectroscopy and differential interference contrast microscopy. J. Bacteriol. 197, 2361–2373. https://doi.org/10.1128/JB.00200-15.
Wang, S., Yu, J., Suvira, M., Setlow, P., Li, Y.q., 2015b. Uptake of and resistance to the antibiotic berberine by individual dormant, germinating and outgrowing Bacillus spores as monitored by laser tweezers Raman spectroscopy. PLoS One 10, e0144183. https://doi.org/10.1371/journal.pone.0144183.
Wen, C., 1969. Coplanar waveguide, a surface strip transmission line suitable for nonreciprocal gyromagnetic device applications. In: 1969 G-MTT International Microwave Symposium. IEEE, pp. 110–115. https://doi.org/10.1109/GMTT.1969.1122668.
Williams, C.F., Lees, J., Lloyd, D., Geroni, G.M., Jones, S., Ambala, S., Baradat, W., Comat, G., Aboubakary, A., Voisin, S., Porch, A., 2018. Real-time microscopic observation of biological interactions with microwave fields. IMBioc 2018 - 2018 IEEE/MTT-S Int. Microwave Biomed. Conf. 1, 199–201. https://doi.org/10.1109/IMBIOC.2018.8428902.
Yang, H., Xiao, X., Zhao, X., Wu, Y., 2017. Intrinsic Fluorescence Spectra of Tryptophan, Tyrosine and Phenyloalanine, p. 102554M. https://doi.org/10.1117/12.2268397.
Zhang, X., Young, M.A., Lyandres, O., Van Duyne, R.P., 2005. Rapid detection of an anthrax biomarker by surface-enhanced Raman spectroscopy. J. Am. Chem. Soc. 127, 4484–4489. https://doi.org/10.1021/ja043623b.
Zhang, P., Kong, L., Setlow, P., Li, Y.q., 2010. Characterization of wet-heat inactivation of single spores of Bacillus species by dual-trap Raman spectroscopy and elastic light scattering. Appl. Environ. Microbiol. 76, 1796–1805. https://doi.org/10.1128/AEM.02851-09.
Zhang, Y., Miao, Z., Huang, X., Wang, X., Liu, J., Wang, G., 2019. Laser tweezers Raman spectroscopy (LTRS) to detect effects of chlorine dioxide on individual nosema bombycis spores. Appl. Spectrosc. 73, 774–780. https://doi.org/10.1177/0003702818817522.